

THERMAL NONLINEARITY EFFECT USED IN LASER EXCITATION OF ULTRASONIC SIGNALS IN GEOMATERIALS

V. N. In'kov,¹ E. B. Cherepetskaya,¹ V. L. Shkuratnik,¹
A. A. Karabutov,² and V. A. Makarov²

UDC 622.611.4:620.179.16

The possibility of creating laser-ultrasonic sources of short power pulses of elastic longitudinal waves on the basis of nonlinear thermal processes in the generator medium is examined theoretically and experimentally. A three-dimensional model of thermal nonlinearity is considered, and the waveforms, spectra, and directional diagrams of signals excited in geomaterials are calculated.

Key words: *thermal nonlinearity, laser excitation, elastic waves, geomaterials.*

Introduction. Ultrasonic methods gain extensive application in solving various geomonitoring problems involving the study of the structure, properties, and state of geomaterials [1]. Simultaneously, practical implementation of the considerable potential of these methods is hampered by the lack of powerful broad-band ultrasonic sources, which would make it possible to examine media with rapid decay of elastic waves on the basis of acoustic spectroscopy principles. The most promising line in the creation of such sources is thermo-optical (laser) excitation of ultrasonic pulses in geomaterials [2].

Laser radiation incident onto the interface between an optically transparent and absorbing media induces local heating of the interfacial layer in the latter medium. Subsequent thermal expansion of this layer results in excitation of elastic waves. If the absorbing medium is a liquid, then only longitudinal waves are generated; if this medium is a solid, then, in addition to longitudinal waves, shear and surface waves can also be excited. The amplitude of the acoustic pressure p_0 is proportional to the volume density of the released heat $w = \mu I_0 \tau_L$ (μ is the absorption coefficient and I_0 and τ_L are the amplitude and duration of the laser pulse, respectively): $p_0 = w\gamma/2$. The factor $\gamma = c_0^2\beta/c_p$ is determined by the velocity of longitudinal elastic waves c_0 and by the thermophysical characteristics of the absorbing medium (β is volume-expansion coefficient and c_p is the specific heat at constant pressure). With the use of pulsed laser excitation of ultrasound, one can generate supershort signals with durations down to 0.1 nsec and pressure amplitudes up to 10 MPa [3]. The possibility of generation of high pressures is primarily related to the use of media with high light-absorption coefficients and very short laser pulses satisfying the condition $\tau_L \ll (\mu c_0)^{-1}$ [4]. The combination of high amplitude and short duration of optic-acoustic signals obtaining record-breaking strain rates. The waveform and spectrum of such acoustic signals can easily be predicted theoretically [5].

A further increase in pressure amplitude of laser-excited ultrasonic pulses (up to 100–1000 MPa) can be achieved by increasing the energy of the light beam. Yet, such an increase results in failure of the medium owing to its overheating, generation of a vapor or plasma, optical breakdown, and other phenomena.

The amplitude of excited acoustic pulses can be increased without damaging the object by using an intermediate liquid absorbing medium covering the object surface and having a maximum value of the parameter γ . Absorbing laser radiation, such a medium undergoes thermal expansion and, thus, generates elastic waves. The medium can be heated by several tens of degrees, so that the temperature dependence of the volume-expansion coefficient starts to affect the ultrasound-generation process. As was shown in the papers [6, 7], which were performed

¹Moscow State Mining University, Moscow 119991. ²International Laser Center, Lomonosov Moscow State University, Moscow 119992; ftkp@mail.ru; aak@sasha.phys.msu.su. Translated from *Prikladnaya Mekhanika i Tekhnicheskaya Fizika*, Vol. 46, No. 2, pp. 179–186, March–April, 2005. Original article submitted July 27, 2004.

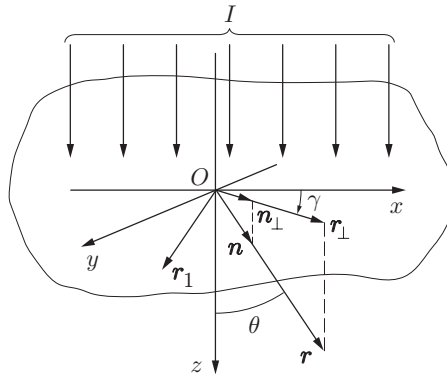


Fig. 1. Thermo-optical excitation of elastic waves in a generator medium.

for a one-dimensional model, allowance for this dependence can increase the signal amplitude almost by an order of magnitude. This effect was called the thermal nonlinearity [7].

In the present work, we consider a three-dimensional theoretical model of laser-ultrasonic sources of powerful broad-band pulses of elastic waves, which are based on the thermal-nonlinearity effect, and results of experimental investigations of such sources.

Theoretical Model. We consider the following model (Fig. 1): a Gaussian light beams is incident onto a planar surface of an absorbing liquid medium ($z > 0$) from air; the light intensity in the beam follows the law $I = I_0 L(t) B(x, y)$, where $L(t) = (\sqrt{\pi})^{-1} \exp[-(t/\tau_L)^2]$ is the time envelope of the laser pulse and $B(x, y) = \exp[-(x^2 + y^2)/r_a^2]$ is the cross-sectional distribution of light in the beam of radius r_a . Let \mathbf{r} and \mathbf{r}_1 be the radius-vectors of the observation point and source point, \mathbf{n} and \mathbf{n}_\perp be the unit vectors, and the angle θ define the direction toward the observation point.

We assume that the light intensity in the absorbing medium obeys the Bouguer law, and the temperature field inside the medium is governed by the heat-conduction equation [4]

$$\frac{\partial T}{\partial t} = \chi \Delta T + \frac{\mu I}{\rho c_p} \exp(-\mu z), \quad (1)$$

where T is the temperature increment, χ , ρ , and μ are the thermal diffusivity, density, and absorption factor of the medium, and $\Delta \equiv \partial^2/x^2 + \partial^2/y^2 + \partial^2/z^2$ is the Laplace operator. Neglecting thermal diffusivity (for water, $\chi = 1.43 \cdot 10^{-7}$ m²/sec), we can write the solution of Eq. (1) in the following dimensionless form:

$$T' = T/T^* = M \exp(-Mz') B(x', y') \Phi(t'). \quad (2)$$

Here $T^* = I_0 \tau_L / (\rho c_p r_a)$ is the normalized temperature, $M = \mu r_a$ is the “optical” thickness of the medium, $\{x', y', z'\} = \{x/r_a, y/r_a, z/r_a\}$ are the dimensionless coordinates, $t' = t/\tau_L$ is the time, and $\Phi(t') = 0.5[1 + \text{erf}(t')]$ is the time dependence of the temperature field in the medium.

As an absorbing medium in subsequent calculations, we take a diluted aqueous solution of Indian ink; in its thermodynamic parameters, this solution is close to water. The absorption factor varies within wide limits, depending on the Indian-ink concentration (from $\mu = 0.1$ cm⁻¹ for water to $\mu > 1000$ cm⁻¹ for pure Indian ink). It is seen from Eq. (2) that the temperature reaches a constant value with time, as it could be expected in the absence of heat conduction. In the case of surface absorption ($M \gg 1$), a thin interfacial layer is heated to a maximum temperature. In the case of volume absorption ($M \ll 1$), uniform heating of the medium is observed. Deeper into the medium, the temperature decays exponentially following the Bouguer law.

Taking into account Eq. (2) and the thermal nonlinearity effect, we can write the inhomogeneous wave equation as

$$\frac{\partial^2 p}{\partial t^2} - c_0^2 \Delta p = \rho c_0^2 \frac{\partial^2}{\partial t^2} [\beta(T) T], \quad (3)$$

where p is the acoustic pressure, $\beta(T)$ is the thermal volume expansion factor nonlinearly depending on temperature, and T_0 is the initial temperature. Below, we restrict ourselves to two first terms in the Taylor series expansion

of $\beta(T)$ in powers of the temperature T : $\beta(T)T = \beta(T_0)T + (d\beta/dT)_{T=T_0}T^2$. We nondimensionalize Eq. (3) using the dimensionless parameters of Eq. (2):

$$\alpha^2 \frac{\partial^2 p'}{\partial t'^2} - \Delta' p' = \frac{\partial^2}{\partial t'^2} \left[\alpha S_1(z') B(x', y') \Phi(t') + \alpha \left(\frac{d\beta}{dT} \right)' S_2(z') B^2(x', y') \Phi^2(t') \right]. \quad (4)$$

Here $p' = p/p_0$, $p_0 = c_0 \beta(T_0) I_0 / c_p$, $\alpha = r_a / (c_0 \tau_L)$ is a parameter that characterizes the ratio between the travel time of sound across the heat-release region to the laser-pulse duration, $S_1(z') = M \exp(-Mz')$, and $S_2(z') = S_1^2(z')$. We have $(d\beta/dT)' = 1.53 \cdot 10^3 \cdot E / r_a$ [J/mm³], where $E = I_0 \tau_L$ is the surface density of the pulse energy.

To solve Eq. (4), we use the time-dependent Fourier transform:

$$p'_\omega(\omega', \mathbf{r}') = \int_{-\infty}^{\infty} p'(t', \mathbf{r}') \exp(i\omega' t') dt', \quad \omega' = \omega \tau_L.$$

This yields the inhomogeneous Helmholtz equation

$$\Delta' p'_\omega + \alpha^2 \omega'^2 p'_\omega = \alpha \omega'^2 [\Phi_\omega(\omega') S_1(z') B(x', y') + \Psi(\omega') (d\beta/dT)' S_2(z') B^2(x', y')], \quad (5)$$

where $\Phi_\omega(\omega') = (i/\omega') L_\omega(\omega') = (i/\omega') \exp(-\omega'^2/4)$ is the spectrum of the function $\Phi(t')$ and $\Psi(\omega') = \int_{-\infty}^{\infty} \Phi_\omega(\Omega) \Phi_\omega(\omega' - \Omega) d\Omega$ is the convolution of the functions. Depending on the proportion between the acoustic

impedances of the transparent and absorbing media, Eq. (5) is supplemented by an appropriate boundary condition: $(\partial p' / \partial z')_{z'=0} = 0$ for the rigid boundary or $p'|_{z'=0} = 0$ for the free boundary. We seek the solution of the Helmholtz equation with the help of the Green function, which has the following form in an unbounded medium:

$$G(\mathbf{r}', \mathbf{r}'_1) = \frac{1}{4\pi |\mathbf{r}' - \mathbf{r}'_1|} \exp(i\alpha \omega' |\mathbf{r}' - \mathbf{r}'_1|). \quad (6)$$

The acoustic pressure spectrum includes a linear component $p'_{\omega,1}$ and a nonlinear component $p'_{\omega,2}$: $p'_\omega(\omega', \mathbf{r}') = p'_{\omega,1}(\omega', \mathbf{r}') + p'_{\omega,2}(\omega', \mathbf{r}')$. For the solution of Eq. (5) with the Green function (6) to satisfy the boundary conditions, this equation needs to be modified by continuing the heat sources $S_{1,2}^c(z')$ into the region $z' < 0$ either evenly [$S_{1,2}^c(z') = S_{1,2}^c(-z')$] in the case of the rigid boundary or oddly [$S_{1,2}^c(z') = -S_{1,2}^c(-z')$] in the case of the free boundary. This yields the solutions

$$p'_{\omega,1}(\omega', \mathbf{r}') = \frac{\alpha \omega'^2 \Phi_\omega(\omega')}{4\pi} \iiint_{-\infty}^{+\infty} dx'_1 dy'_1 dz'_1 B(x'_1, y'_1) S_1^c(z'_1) F(\alpha, \omega', \mathbf{r}, \mathbf{r}'); \quad (7)$$

$$p'_{\omega,2}(\omega', \mathbf{r}') = \frac{\alpha \omega'^2 (d\beta/dT)' \Psi(\omega')}{4\pi} \iiint_{-\infty}^{+\infty} dx'_1 dy'_1 dz'_1 B^2(x'_1, y'_1) S_2^c(z'_1) F(\alpha, \omega', \mathbf{r}, \mathbf{r}'), \quad (8)$$

where

$$F(\alpha, \omega, \mathbf{r}, \mathbf{r}') = \frac{\exp(i\alpha \omega' [(x' - x'_1)^2 + (y' - y'_1)^2 + (z' - z'_1)^2]^{1/2})}{[(x' - x'_1)^2 + (y' - y'_1)^2 + (z' - z'_1)^2]^{1/2}}.$$

Expressions (7) and (8) are expansions of the acoustic field by diverging spherical waves. A complex regime of running and standing waves is observed in the region of action of heat sources, and only at distances exceeding μ^{-1} does a pure running wave propagate. Therefore, we use the far wave zone approximation ($|\mathbf{r}'_1| \ll |\mathbf{r}'|$), for which the Green function acquires the form

$$G(\mathbf{r}', \mathbf{r}'_1) \approx \frac{1}{4\pi |\mathbf{r}'|} \exp(i\alpha \omega' |\mathbf{r}'|) \exp \left[-i\alpha \omega' \frac{(\mathbf{r}' \mathbf{r}'_1)}{|\mathbf{r}'|} \right]. \quad (9)$$

We substitute Eq. (9) into Eqs. (7) and (8) to obtain

$$p'_{\omega,1}(\omega', \mathbf{r}') = \frac{\alpha \omega'^2 \Phi_\omega(\omega')}{4\pi |\mathbf{r}'|} \exp(i\alpha \omega' |\mathbf{r}'|) \iiint_{-\infty}^{+\infty} B(\mathbf{r}'_{1\perp}) S_1^c(z'_1) \exp(-i\alpha \omega' (\mathbf{n} \mathbf{r}'_1)) d\mathbf{r}'_{1\perp} dz'_1; \quad (10)$$

$$p'_{\omega 2}(\omega', \mathbf{r}') = \frac{\alpha\omega'^2(d\beta/dT)'\Psi(\omega')}{4\pi|\mathbf{r}'|} \exp(i\alpha\omega'|\mathbf{r}'|) \int_{-\infty}^{+\infty} \int_{-\infty}^{+\infty} B^2(\mathbf{r}'_{1\perp}) S_2^c(z'_1) \exp(-i\alpha\omega'(\mathbf{n}\mathbf{r}'_1)) d\mathbf{r}'_{1\perp} dz'_1. \quad (11)$$

Here $\mathbf{n} = \mathbf{r}'/|\mathbf{r}'|$ is a unit vector directed toward the observation point (see Fig. 1). As the condition $\mathbf{k}'\mathbf{r}' = \alpha\omega'\mathbf{r}' \gg 1$ is satisfied in the far wave zone, expressions (10) and (11) take the following form:

$$p'_{\omega,1}(\omega', \mathbf{r}') = \frac{\alpha\omega'^2\Phi_\omega(\omega')}{4\pi|\mathbf{r}'|} \exp(i\alpha\omega'|\mathbf{r}'|) \int_{-\infty}^{+\infty} B(\mathbf{r}'_{1\perp}) \exp(-i\alpha\omega'(\mathbf{n}_\perp\mathbf{r}'_{1\perp})) d\mathbf{r}'_{1\perp} \\ \times \int_{-\infty}^{+\infty} S_1^c(z'_1) \exp(i\alpha\omega'z'_1 \cos \theta) dz'_1; \quad (12)$$

$$p'_{\omega,2}(\omega', \mathbf{r}') = \frac{\alpha\omega'^2(d\beta/dT)'\Psi(\omega')}{4\pi|\mathbf{r}'|} \exp(i\alpha\omega'|\mathbf{r}'|) \int_{-\infty}^{+\infty} \int_{-\infty}^{+\infty} B^2(\mathbf{r}'_{1\perp}) \exp(-i\alpha\omega'(\mathbf{n}_\perp\mathbf{r}'_{1\perp})) d\mathbf{r}'_{1\perp} \\ \times \int_{-\infty}^{+\infty} S_2^c(z'_1) \exp(i\alpha\omega'z'_1 \cos \theta) dz'_1. \quad (13)$$

Here $\mathbf{n}_\perp = \mathbf{r}_\perp/|\mathbf{r}_\perp| = \mathbf{n} \sin \theta$. After calculating the integrals in Eqs. (12) and (13), we obtain the following relations for the Gaussian beam:

$$p'_{\omega,1}(\omega', \mathbf{r}') = \begin{cases} M^2\alpha\omega'^2\Phi_\omega(\omega')H/2|\mathbf{r}'|(M^2 + \alpha^2\omega'^2 \cos^2 \theta), \\ M\alpha^2\omega'^3 \cos \theta\Phi_\omega(\omega')H/2|\mathbf{r}'|(M^2 + \alpha^2\omega'^2 \cos^2 \theta) \end{cases}$$

for the rigid boundary and

$$p'_{\omega,2}(\omega', \mathbf{r}') = \begin{cases} M^3\alpha\omega'^2(d\beta/dT)'\Psi(\omega')H/2|\mathbf{r}'|(4M^2 + \alpha^2\omega'^2 \cos^2 \theta), \\ iM^2\alpha^2\omega'^3 \cos \theta (d\beta/dT)'\Psi(\omega')H/4|\mathbf{r}'|(4M^2 + \alpha^2\omega'^2 \cos^2 \theta) \end{cases}$$

for the free boundary [$H = \exp(i\alpha\omega'|\mathbf{r}'| - (1/2)i\alpha^2\omega'^2 \sin^2 \theta)$].

Numerical Calculation. In numerical calculations, we used the above-listed physical characteristics of the aqueous Indian-ink solution and the following characteristics of laser radiation, which can be obtained on a GEOSCAN-02M laser-ultrasonic setup intended for characterizing geomaterials: $\lambda = 1.06 \mu\text{m}$, $\tau_L = 10^{-8}$ sec, $r_a = 1\text{--}10$ mm, and $E_{\max} = 260$ mJ/cm².

Figure 2 shows the time profiles of the linear and nonlinear components of the acoustic signal for the rigid and free boundaries ($\tau' = t' - \alpha r'$ is the dimensionless time in the “running” coordinate system). The calculations were performed for the point with the coordinate $z' = 10$ at the beam axis for $r_a = 1$ mm, $M = 200$ cm⁻¹, and $E = 210$ mJ/cm². Under these conditions, the local temperature increase in the medium is 10 K, which allows us to use the far wave zone approximation, where a bipolar pulse consisting of compression and rarefaction phases is formed in the case of the rigid boundary (Fig. 2a) and a tripolar pulse (two compression phases and a rarefaction phase) is formed in the case of the free boundary (Fig. 2b). The nonlinear component of the signal occurs with some delay after the linear one, which, together with diffraction, results in an asymmetric waveform of the acoustic pulse. For the nonlinear contribution to be comparable with the linear contribution under identical conditions, the case of the rigid boundary requires a lower density of the laser-pulse energy, as compared to the free boundary. The duration of the acoustic signal is determined by the “optical” thickness of the medium. The greater the value of M , the shorter the pulse.

The components of the acoustic signal also differ in their duration; this circumstance is reflected in their spectra (Fig. 3) predicted for the values of parameters that were used to calculate the dependences in Fig. 2b. The absolute values of the spectra are normalized to their maximum values. The spectrum of the nonlinear signal is wider than the spectrum of the linear signal, and a more broad-band signal is excited in the case of the free boundary.

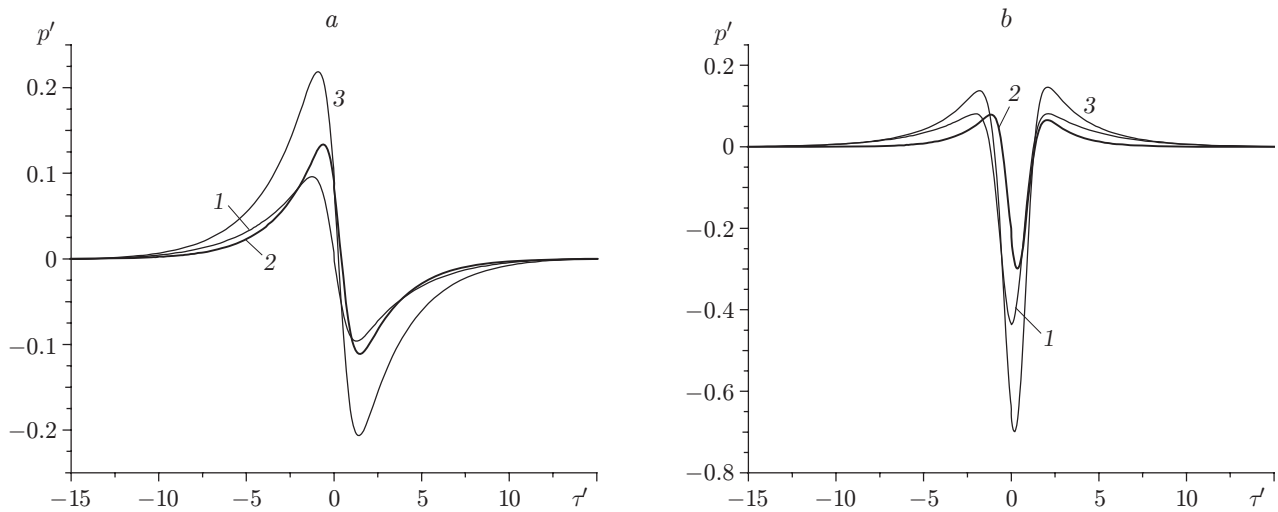


Fig. 2. Pressure increment versus time in the “running” coordinate system in the cases of the rigid boundary (a) and the free boundary (b) for the linear (1) and nonlinear (2) components of the optical-acoustic signal and the sum of these components (3).

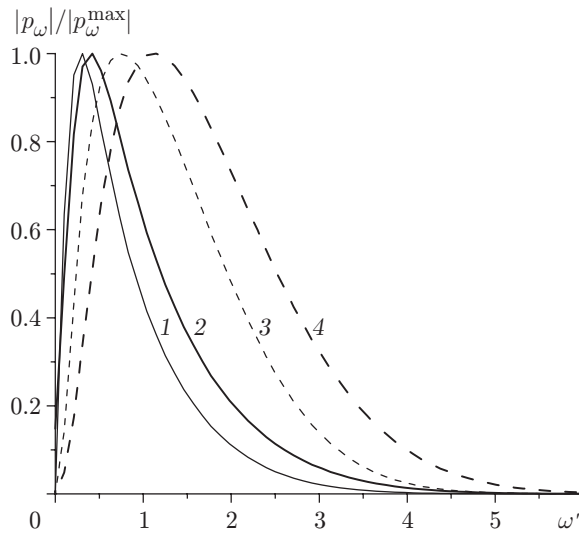


Fig. 3. Absolute values of the amplitude spectra of the linear (1 and 3) and nonlinear (2 and 4) components of the optical-acoustic signals in the cases of the rigid (curves 1 and 2) and free (curves 3 and 4) boundaries.

Figure 4 shows the directional diagrams of the acoustic field versus the parameter M and for two types of boundary conditions. For $M = 20$, a thin disk-shaped surface layer of the medium is heated (surface absorption, curve 1), which subsequently excites an acoustic wave. For $M = 0.2$, volume absorption is observed (curves 4 and 5), resulting in almost uniform heating of the medium over its depth, and the source of the acoustic wave is a cylindrical heat-release region. Curves 2 and 3 describe an intermediate case ($M = 2$). For identical parameters of the laser beam, the directional diagrams predicted in the case of surface absorption for the rigid and free boundaries are almost coincident. Simultaneously, in the case of volume absorption, the directional diagram for the rigid boundary is much wider than that for the free boundary.

Experiment. To verify the dependence of the amplitude of the optical-acoustic signal on the surface density of laser-pulse energy, we performed an experiment. Elastic waves were excited in the aqueous solution of Indian ink contained in a diaphragm (cylinder) 10 mm high and 20 mm in diameter, which was placed on the surface

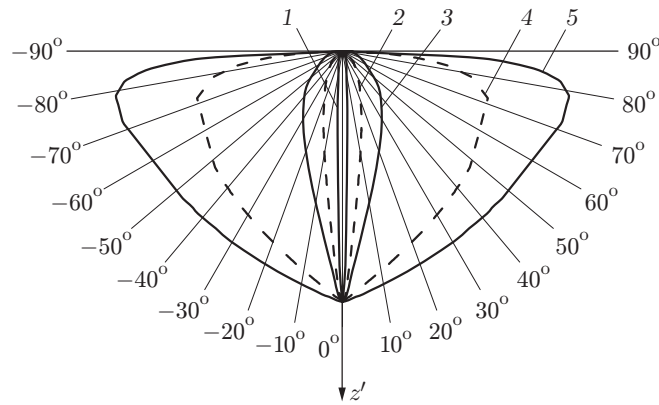


Fig. 4. Directional diagrams of the thermal sources of sound in the cases of the rigid and free boundaries (solid and dashed curves, respectively) for $M = 20$ (1), 2 (2 and 3) and 0.2 (4 and 5).

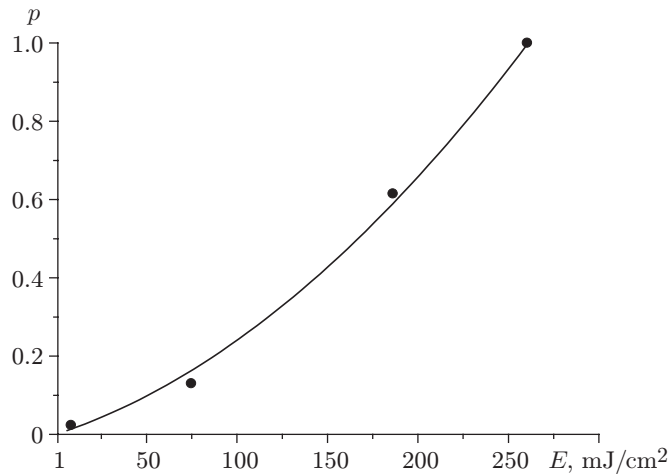


Fig. 5. Amplitude of the acoustic signal excited in the aqueous solution of Indian ink versus the surface density of laser-pulse energy: the curve is the predicted dependence and the points are the experimental data.

of the detector. For this concentration of Indian ink, the absorption coefficient μ determined experimentally from the leading front of the acoustic signal was 345 cm^{-1} . From above, the cylinder was covered by a glass plate to obtain an almost rigid boundary (the ratio between the acoustic impedances of water and glass is 0.11). A diafragma prepared from blackened heavyweight paper was used to form a laser beam with a radius of 4 mm. The source of light pulses was the solid laser of the GEOSCAN-02M setup. The laser-pulse energy was varied by the use of different combinations of light filters. Figure 5 shows the predicted pressure-pulse amplitude versus the surface density of laser-pulse energy and the experimental data. The amplitude of the acoustic signal normalized to its maximum value increases nonlinearly with increasing energy density (quadratic dependence). The experimental points lie fairly close to the predicted curve, the maximum deviation being within 15%. It was also found that an increase in laser-pulse energy is accompanied not only by a profound increase in the amplitude of the acoustic signal but also by an increase in its spectral width (approximately by a factor of 1.5).

Conclusions. The presented calculations and experimental data prove the possibility of increasing the intensity and width of the spectrum of ultrasonic signals excited by laser radiation in a geological medium with a high damping factor of elastic waves. Such a possibility is ensured by the thermal-nonlinearity effect observed in a generator medium whose optical absorption factor is of the order of 10^3 cm^{-1} and the temperature volume-expansion factor is of the order of 10^{-4} K .

This work was supported by the Foundation “Leading Scientific Schools in Russia” (Grant No. NSH-1467.2003.5).

REFERENCES

1. I. N. Ermolov, *Theory and Practice of Ultrasonic Monitoring* [in Russian], Mashinostroenie, Moscow (1981).
2. A. A. Karabutov, V. A. Makarov, V. L. Shkuratnik, and E. B. Cherepetskaya, “Theoretical estimate of parameters of laser-excited ultrasonic pulses in geomaterials,” *Fiz.-Tekh. Probl. Razrab. Polezn. Iskop.*, No. 4, 11–18 (2003).
3. A. A. Karabutov, V. V. Murashov, and N. B. Podymova, “Laser optical acoustic transducers for inspection of layered composites,” *Mech. Compos. Mater.*, **35**, 125–134 (1999).
4. V. É. Gusev and A. A. Karabutov, *Laser Optoacoustics* [in Russian], Nauka, Moscow (1991).
5. L. V. Burmistrova, A. A. Karabutov, A. I. Portnyagin, et al., “Method of transfer functions in thermo-optical excitation of sound,” *Akust. Zh.*, **24**, No. 5, 655–663 (1978).
6. T. A. Dunina, S. V. Egerev, L. M. Lyamshev, and K. A. Naugol’nykh, “On the nonlinear theory of the thermal mechanism of sound generation by laser radiation,” *Akust. Zh.*, **25**, No. 4, 622–625 (1979).
7. L. V. Burmistrova, A. A. Karabutov, O. V. Rudenko, and E. B. Cherepetskaya, “Effect of thermal nonlinearity on the thermo-optical generation of sound,” *ibid.*, pp. 616–619.